IOSR Journal Of Applied Physics (IOSR-JAP)
e-ISSN: 2278-4861.Volume 12, Issue 2 Ser. I (Mar. – Apr. 2020), PP 01-06
www.Iosrjournals.Org

Optical Properties of ZnO Nonostructures Synthesised Using Different Concentrations of Zinc Acetate

[1] A. B. Awatif, [2]Mubarak Dirar Abdallah, [3] E.M. Elssfah [4] Abdalsakhi S M.H ,
[1,2] Sudan University of Science &Technology-College of Science-Department of Physics-Khartoum- Sudan
[3] Gadarif University Faculty of Engineering-Department of Physics –Gadarif-Sudan
[4] Al-Neenlen University – Faculty of Science and Technology Department of Physics- Khartoum- Sudan

Abstract: *Thin films of Zinc Oxide nonostructures have been prepared by simple method and using spin coating technique deposited on ITO glass substrate. The study used different molars of zinc acetate 0.1 ,0.2 ,0.3 ,0.4 ,0.5 ,0.6 ,0.7 ,0.8 ,0.9 and1.0. The optical properties; including absorption coefficient, refractive index and energy bandgap were investigated by means of absorption, transmittance and reflectance spectra. Although, the refractive index has uncharacteristic behavior in the wavelength at the range 306 - 344 nm, the result showed the average value of refractive index for all samples is equal to 2.159. Also, the result confirmed that the nanostructure with concentration of 1.0 molar has lowest energy bandgap 3.44 eV and this may leed to highest coductivity comparing with other concentrations. This entire advantage make ZnO nanostrucures syntheised with 1.0 moalr of zinc acetate have wide range for solar cell applications.*

Keyword: *ITO glass substrate, thin film , nanostructures, Optical properties.*

Date of Submission: 26-02-2020 Date of Acceptance: 09-03-2020

I. Introduction

Among metal oxide semiconductors, ZnO is increasingly recognized as a suitable alternative due to its richest range of morphologies among the wide band gap semiconductors (3.37 eV) and relatively lower cost of production [1,2]. ZnO was also reported to exhibit higher quantum efficiency and photocatalytic activity than TiO^2 in certain cases [3].

The correlation between the properties of solids and their size and shape on atomic scale has been exploited for decades and it is well-established that nanostructure systems encompass a varied range of materials and/or devices that show various phenomena which is controlled by the manipulation of their microstructure on atomic scale. Therefore, it has been demonstrated that ZnO nanostructures exhibited antimicrobial activity against on a broad spectrum of bacteria including staphylococcus auerus [4] and Escherichia coli [5,6,7]. ZnO nanoparticles seem to have relative toxicity to bacteria but exhibit minimal effect on human cells [4]. The disruption of the cell membrane is attributed to per-oxidation of the unsaturated phospholipids due to photo-catalytically induced hydrogen peroxide [8]. Cell membrane and wall damage upon the contact with ZnO nanoparticles occur to inhibit bacterial growth [4,5]. In addition, binding Zn^{2+} ion to the membranes of microorganisms results in prolong the lag phase of the microbial growth cycle [9]. A recent toxicology study by Poynton et al. [10,11] suggested that both ZnO nanoparticles and Zn^{2+} are toxic, but have different modes of action.

ZnO nanostructures has many potential applications, such as light emitting lasers and diodes, piezoelectric devices and photo catalysts [12, 13], gas and chemical sensors [14], solar cell [15], ultraviolet detector [16] and biomolecular sensors [17]. ZnO nanoparticles are also generally recognized as safe and biocompatible and have been used as drug carriers and medical filling materials [18]. Many methods have been developed to synthesize ZnO nanoparticles with different sizes and morphologies.The deposition of high quality ZnO thin films is reported using a wide variety of techniques, such as, sputtering [19], chemical vapor deposition [20], spray pyrolysis [21], sol-gel method [22], and electrochemical deposition [23]. The sol- gel chemical /deposition technique is very attractive as it can be entrenched easily in laboratory for the deposition of semiconducting thin films [20].

In this study, a sol-gel method has been used to prepare a solution of ZnO. Then ZnO/solution deposited on glass substrates by using spin coating technique to prepare ZnO/ITO films nanoparticles with the use of different concentrations /molar of zinc acetate. Moreover, the effects of the different concentrations on the structural and the electrical conductivity were investigated. The most important advantages of this approach , in comparison the different of the molar concentration on the electrical properties of ZnO nanostructure. The samples were characterized by XRD, FTIR and UV-visible spectroscopy.

Samples Preparation:

The precursors that utilized to synthesize ZnO nanostructures by using different concentration molars seed layers and by sol-gel process are Zinc acetate dehydrate $Zn(CH_3COOH)_2.2H_2O$. The need for surfactant is fulfilled by the use of 2-methoxyethanol (ME) $CH_3OCH_2CH_2OH$. The stock solution for the samples was prepared by using Zinc acetate in different molar (0.1.0 ,0.2 ,0.3 , 0.4 ,0.5 ,0.6 , 0.7 ,0.8 ,0.9 and 1.0 molar). Each molar of zinc acetate was dissolved in 100 ml of ethanol in the glass beaker. Then these solution were stirred for 60 min at 80°C to get milky solution. Then some drops of 2-methoxyethanol (ME) was added carefully to the milky solution as stabilizer to obtain a transparent solution. Finally the Zinc oxide solution has been got. The ten mounts of the samples have been leaved in the laboratory at room temperature for about 24 hours. Then the samples were washed by distilled water to obtain the Sol. The sol-gel for each sample was used to prepare the film by spinner (spin coating). The films were prepared in ITO glass slide. The ITO glass were cleaned with ethanol before, washing with deionizer water and acetone. The coating of the films on ITO glass was performed at room temperature, with suitable speed rate for 60 s. The optical conductivity and electrical conductivity of ZnO thin films sample were measured as a function of wavelength by UV-visible spectroscopy. The Fourier Transform Infrared Spectrophotometer (FTIR) in the range of 400 to 4000 cm^{-1} used to recorde some location of the band positions(spinel structure) as wavenumber function. The crystal structure of the samples were characterized at room temperature by using a Philips PW1700 X-ray diffract meter .

II. Results and Discussion:

Figure (1) shows the relation between the absorbance and the wavelengths of the ten samples of ZnO /TIO nanostructures using different concentrations of zinc acetate as follow: 1.0 ,0.9, 0.8 ,0.7 ,0.6 ,0.5 ,0.4 ,0.3 ,0.2 and 0.1 in molar respectively. As can be seen that the absorbance spectra for all samples of as-synthesised ZnO thin films nanostructures have one broad absobance band at 266 nm and this may atrributed to the reduction in crystallite size of the spinal cubic structure. Moreover , Figure (1) indicates that the absorbance of ZnO thin films nanostrucures are gradually increase with increasing of zinc acetate concentrations. This is because the addition of zinc acetate in each sample will help the as-synthesied ZnO thin films nanostructures to absorb the incident radiation by its free electrons.

The transimittance spectra of the ten samples of the ZnO thin film nanostructures in the range of 120 - 720 nm were investigated via UV-visible spectroscopy (Fig.2). The results exhibted that all samples that were prepared using different concentrations of zinc acetae reached a saturation before 276 nm and the average transmittance value of the samples equal 1.495 a.u . Figure (2) also showed that the transmittance spectra value will decrease with increasing of zinc acetae concentration.

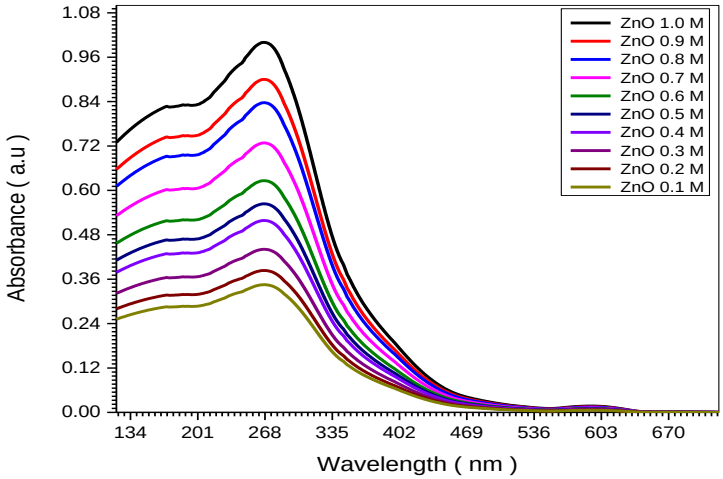

Figure (1): shows the relation between absorbance and wavelengths of the ten samples of as-synthesised ZnO thin film nanostructures.

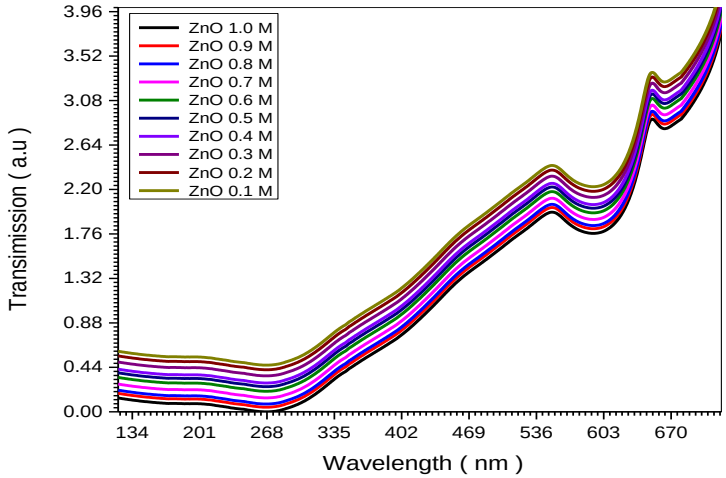

Figure(2): indicates the relation between transimission and wavelengths of the ten samples of as-synthesised ZnO thin film nanostructures.

Figure (3) shows the reflectance spectra of the ten samples of as-synthesised ZnO nanostructures at different concentrations of zinc acetate. The spectrum extended from 134 to 410 nm. The Figure represented that the reflectance at particular wavelength 345 nm can be shifted to blue spectrum when decreasing the concentration of zinc acetate and that means at high concentrations of zinc acetate the ZnO nanoparticles are almost uniformly distributed in the sample.

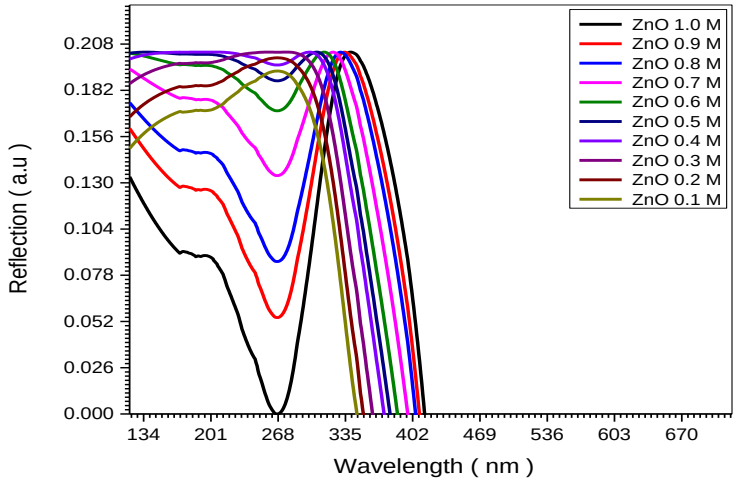

Figure (3): shows the reflectance spectrum of the ten samples that made of as-synthesised ZnO nanostructues.

The absorption coefficient (α) of the samples of as-synthesised ZnO films nanostructures can be obtained by using the Beer-lambert's relation:

$$\alpha = \frac{2.303xA}{t} \qquad (1)$$

where (A) is the absorbance and (t) is the thickness of the film. Figure (4) shows a relating ploting graph between (α) and the wavelength (λ) of ten samples of ZnO nanostructures. The results indicate a maximum value of $\alpha = 4.63x10^3$ cm^{-1} materialized in the U.V region 270 nm at concentration of 1.0 moalr of zinc acetate where the absorption coefficient dcreases to $\alpha = 1.11x10^3$ cm^{-1} for low concentration of 0.1 molar of zinc acetate. High value of absorption coefficient means that the transition must corresponding to a direct electronic transition, and the properties of this state are important since they are responsible for electrical conduction.

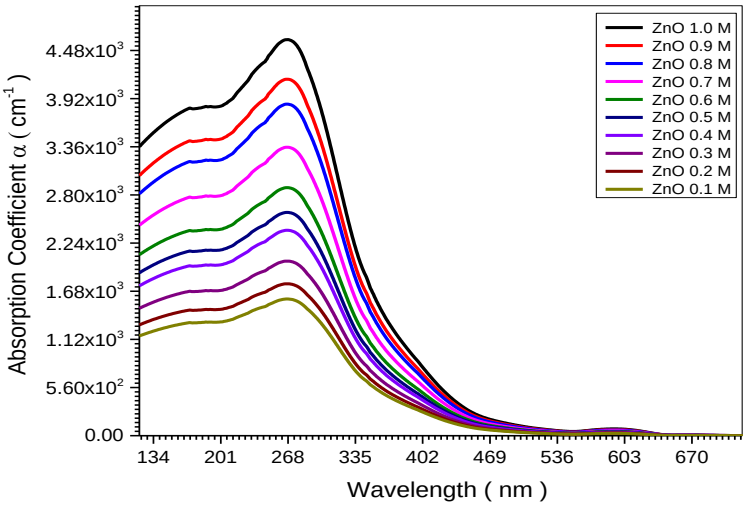

Figure(4): represented the relation between absorption coefficient and wavelengths of as-synthesised ZnO nanostructures.

The refractive index (n) plays a very important role in optical communication and for designing the optical devices. The refractive index (n) can be calculated by usig the following relation:

$$n = \left[\left(\frac{(1+R)}{(1-R)} \right)^2 - (1 + k^2) \right]^{\frac{1}{2}} + \frac{(1+R)}{(1-R)} \qquad (2)$$

where (R) is the reflectivity and k is the extinction coefficient where. $k = \frac{\alpha\lambda}{4\pi}$. Figure (5) shows the refractive index (n) of as-synthesised ZnO nanostructures film as a function of wavelength. Figure (5) confirmed that at range of 422 - 469 nm all curves of the refractive index of the samples represented a macximum peak at n = 2.159, and this result nearly agree with standard refractive index n= 2.004 of ZnO [24]. Also the result demonstrated that the value of (n) begins to decrease between the wavelengths 306 - 344 nm at the region of spectrum. This behavior may due to the nature of the sharp absorption of Zinc Oxide nonostructurs that leads to an electronic transmission at the absorption edge of 4.66 eV.

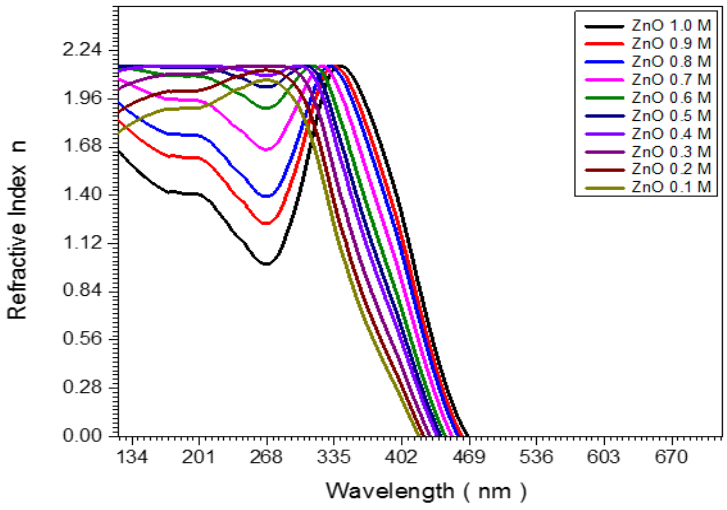

Figure (5): represent the refractive index of the ten samples of as-synthesised ZnO nanostructures as function of wavelength.

The optical energy gap E_g has been calculated by using the following relation:

$$(\alpha h\upsilon)^2 = C(h\upsilon - E_g) \quad (3)$$

where **α** is the absorption coefficient , C is constant and E_g is the bandgap energy. The direct bandgap energies were determined for the different concentrations of zinc acetate of as-synthesised ZnO thin films nanostructures by plotting $(\alpha h\upsilon)^2$ versus photon energy (hυ) curves as shown in Figure (6). The bandgap of ZnO films was stimated from the interception between the tangent to the linear portion of the curve and hυ axix (figure 6). The results indicated that the ZnO film nanostructures that synthzised by using 0.1 molar of zinc acetate has highest bandgap (3.889) eV), whereas those synthezised by using 1.0 molar exhibted lowest bandgap (3.443 eV), which believed to possess a better coductivty [25]. Also, the as-synthezised ZnO nanostructures possessed a significantly higher bandgap enegy, or showed a redshift from 0.16 (for 1.0 molar) to 0.28 ev (for 0.1 molar) comparing to the bandgap of bulck ZnO 3.6 eV. This shift can be attributed to quntum confinement effect of the formatin of ZnO nanostructures.

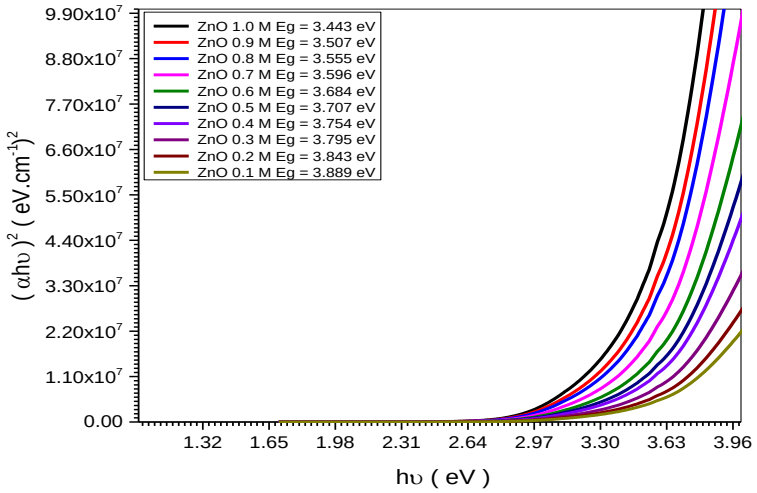

Figure (6): Plot of $(\alpha h\upsilon)^2$ versus the photon energy (**hυ**) for ZnO nanostructure synthezised by using different concentrations of zinc acetate.

III. Conclusion:

In this dtudy ZnO film nanostructures were synthesised by using a sol-gel method. Although the result demonstrateed a broad absobance band at 266 nm, the absorbance of ZnO thin films nanostrucures were gradually increased with increasing of zinc acetate concentrations.The value of absorption coefficient (α) equal to $4.63x10^3$ m^{-1} for all samples in the U.V region at wavelength 270 nm. The result revealed that the optical bandgap of as-synthezised ZnO nanostructure were affected by the difference of the concentrations of zinc acetate. The nanostructure with concentration of 1.0 molar have the highest absorbtion and lowest energy gap 3.44 eV and this leed to highest coductivity. This entire advantage make ZnO nanostrucures that syntheised with 1.0 moalr of zinc acetate have wide range for solar cell applications.

Reference

[1]. O. Seven, B. Dindar, S. Aydemir, D. Metin, M.A. Ozinel, S. Icli, Solar photocatalytic disinfection of a group of bacteria and fungi aqueous suspensions with TiO2, ZnO and Sahara desert dust, J. Photochem. Photobiol. A Chem. 165 (2004) 103−107.

[2]. Attarad Ali, HiraZafar, Muhammad Zia, IhsanulHaq, Abdul RehmanPhull, JohamSarfraz Ali, AltafHussain (2016), Synthesis, characterization, applications, and challenges of iron oxide nanoparticles, Nanotechnology, Science and Applications , Volume (9), pages (49–67).

[3]. Fox, M., Optical Properties of Solids, Oxford University Press, New York, 2001.

[4]. Gupta,M.C.,andJ.Ballato,The Handbook of Photonics, 2nd edition, CRC Press, Boca Raton, FL, 2007.

[5]. Rogers, A., Essentials of Photonics+, 2nd edition, CRC Press, Boca Raton, FL, 2008.

[6]. Kingery,W. D., H. K. Bowen, and D. R. Uhlmann ,Introduction to Ceramics, 2nd edition, Wiley,New York, 1976, Chapter 13.

[7]. Saleh, B. E. A., and M. C. Teich, Fundamentals ofPhotonics, 2nd Edition, Wiley, Hoboken,NJ, 2007.

[8]. U. Ozgur, Ya I. Alivov, C. Liu, A. Teke, M.A. Reshchikov, S. Dog˘an, V. Avrutin, S.-J.Cho, H. Morkoc, A comprehensive review of ZnO materials and devices, J. Appl.Phys. 98 (2005) 041301.

[9]. J. Yu, X. Yu, Hydrothermal synthesis and photocatalytic activity of zinc oxide hollow spheres, Environ. Sci. Technol. 42 (2008) 4902−4907.

[10]. N. Talebian, M.R. Nilforoushan, E. Badri Zargar, Enhanced antibacterial performance of hybrid semiconductor nanomaterials: ZnO/SnO2 nanocomposite thin films, Appl. Surf. Sci. 258 (2011) 547−555.

[11]. J. Sawai, S. Shoji, H. Igarashi, A. Hashimoto, T. Kokugan, M. Shimizu, H. Kojima, Hydrogen peroxide as an antibacterial factor in zinc oxide powder slurry, J. Ferment. Bioeng. 86 (1998) 521−522.
[12]. Kim K, Moon T, Lee M, Kang J, Jeon Y, Kim S: Light-emitting diodes composed of n-ZnO and p-Si nanowires constructed on plastic substrates by dielectrophoresis. Solid State Sci, 13 (2011) 1735–1739.
[13]. Kim H, Gilmore CM, Transparent conducting aluminum-doping zinc oxide thin filims for organc light emitting devices , Appl. Phys. Lett., 76 (2000) 259-264.
[14]. Foo KL, Kashif M, Hashim U, Ali M: Fabrication and characterization of ZnO thin films by sol–gel spin coating method for the determination of phosphate buffer saline concentration. Curr Nanosci, 9 (2013) 288–292.
[15]. Guillen E, Azaceta E, Peter LM, Zukal A, Tena-Zaera R, Anta JA: ZnO solar cells with an indoline sensitizer: a comparison between nanoparticulate films and electrodeposited nanowire arrays. Energy Environ Sci 2011, 4:3400–3407.
[16]. Chai G, Lupan O, Chow L, Heinrich H: Crossed zinc oxide nanorods for ultraviolet radiation detection. Sensor Actuat A Phys 2009, 150:184–187.
[17]. Fulati A, Ali SMU, Asif MH, Alvi NH, Willander M, Brännmark C, Strålfors P, Börjesson SI, Elinder F, Danielsson B: An intracellular glucose biosensor based on nanoflake ZnO. Sensor Actuat B Chem 2010, 150:673–680.
[18]. Mirhosseini M, Firouzabadi FB (2013) Antibacterial activity of zinc oxide nanoparticle suspensions on food-borne pathogens. Int J Dairy Technol 66(2):291–295
[19]. Li YB, Bando Y, Sato T, Kurashima K: ZnO nanobelts grown on Si substrate. ppl Phys Lett 2002, 81:144–146.
[20]. Lee W, Sohn H, Myoung JM: Prediction of the structural performances of ZnO nanowires grown on GaAs (001) substrates by metalorganic chemical vapour deposition (MOCVD). Mater Sci Forum 2004, 449–452:1245–1248.
[21]. Karami H, Fakoori E: Synthesis and characterization of ZnO nanorods based on a new gel pyrolysis method. J Nanometer 2011, 2011:11.
[22]. Kaneva N, Dushkin C: Preparation of nanocrystalline thin films of ZnO by sol–gel dip coating. Bulg Chem Commun 2011, 43:259–263.
[23]. Yi S-H, Choi S-K, Jang J-M, Kim J-A, Jung W-G: Low-temperature growth of ZnO nanorods by chemical bath deposition. J Colloid Interface Sci 2007, 313:705–710.
[24]. Fan, Z., & Lu, J. Zinc Oxide Nanostructured : Synthesis and Properties. Journal of Nanoscience and Nanotechnology, (2005) 1561-1573.
[25]. A.F. Mansour, S.F. Monsour and M.A. Abdo, Improvement Structural and Optical Properties of ZnO/PVA nanocomposites, 2015, 11: 60-69.

A. B. Awatif, etal. "Optical Properties of ZnO Nonostructures Synthesised Using different Concentrations of Zinc Acetate." *IOSR Journal of Applied Physics (IOSR-JAP)*, 12(2), 2020, pp. 01-06.